

Adil Kadyrov - Akbope Karsakova - Bakytzhan Donenbayev - Kyrmyzy Balabekova

# ESTABLISHING THE STRENGTH CHARACTERISTICS OF THE LIFTING-LEVELING DEVICE STRUCTURES OF THE VPO-3-3000 MACHINES FOR THE TRACK STRAIGHTENING

*This article deals with replacement of the magnetic grippers on the VPO-3-3000 machines with roller grippers. The novelty lies in establishment of dependences characterizing stress and strain in elements of the lifting and straightening devices and in rails during the operation. Reliability of the program for calculating the structural parameters of the lifting and straightening device for the VPO-3-3000 track renewal machine is shown. The developed design of the lifting and straightening device makes it possible to select the rational parameters of technology and the operating mode of the device. This design is recommended for use when developing working bodies for the straightening machines. The article presents calculation of the lifting and straightening device structural elements' strength during operation, in the Ansys WB software package.*

**Keywords:** railway track, tamping, ballast, roller rail gripper, track repair

## 1 Introduction

Railway ballast is the railway track foundation that is composed of graded stone ballast. The increasing flow of rail transport may inevitably deform or damage the railway line. In order to ensure the train safety, smoothness and fast running, as well as to extend the service life of various components of the railway track, the maintenance work of the line needs to be done timely to keep the line equipment in good condition [1-3].

At the moment, one of the main areas of resource-saving technologies used in repairing the railway track is the deep cleaning of the gravel ballast layer [4].

The quality of leveling is determined by requirements for the accuracy of positioning a railway track in terms of level, longitudinal section and plan. Quantitative values of these requirements are established and determined by applicable technical regulations [5].

The tamping operation is a continuous cycle process. The cycle itself has five phases: the first phase is that the tamping tines are inserted into the ballast around the sleepers, the second phase is that the tamping tines squeeze the ballast to fill the voids under the sleeper, the third phase is keeping the squeezing, the fourth phase is loosening the squeezing and the fifth phase is that the tamping tines are removed, as well as the tamping tines always maintain the vibration throughout the tamping operation process [6-10].

The dense train schedules, often with intermittent inter-train intervals, make it necessary to carry out track

work within short periods of time. Despite this, in the areas of heavy freight or high-speed passenger train circulation, requirements for stability of the rail track parameters and strength characteristics of the track must be observed, which makes it necessary to introduce the latest track-and-field resource-saving technologies.

The degree of the ballast layer consolidation corresponds to its greatest bearing capacity and resistance to a shape change. Information about the degree of the ballast consolidation under sleepers is important because it gives the possibility to evaluate the quality of the repair works, as well as further deformation of the track geometry. As studies show [11-14], a well-consolidated ballast layer after the track repair enables to extend the lifecycle period of the ballasted track and track structures significantly.

In the course of the railway track operation, the ballast is clogged. The pores between the gravel particles are filled with weeds. The simultaneous moistening and contamination of the ballast leads to formation of a kind of grease between the gravels. As a result, the ballast layer loses its bearing capacity.

## 2 Machine park of the Akadyr mechanized distance

In the network of Kazakhstan railways, more than 55 track renewal trains VPO-3-3000, for track straightening and ballast compaction after deep cleaning, are used.

The track renewal machine VPO-3-3000 produced by the Tulazheldormash plant CJSC, is used for all the

Adil Kadyrov<sup>1</sup>, Akbope Karsakova<sup>1</sup>, Bakytzhan Donenbayev<sup>1</sup>, Kyrmyzy Balabekova<sup>2,\*</sup>

<sup>1</sup>Karaganda State Technical University, Karaganda city, Republic of Kazakhstan

<sup>2</sup>L.N. Gumilyov eurasian national university, Nur-Sultan city, Republic of Kazakhstan

\*E-mail of corresponding author: 06\_03\_92@mail.ru



This is an open access article distributed under the terms of the Creative Commons Attribution 4.0 International License (CC BY 4.0), which permits use, distribution, and reproduction in any medium, provided the original publication is properly cited. No use, distribution or reproduction is permitted which does not comply with these terms.

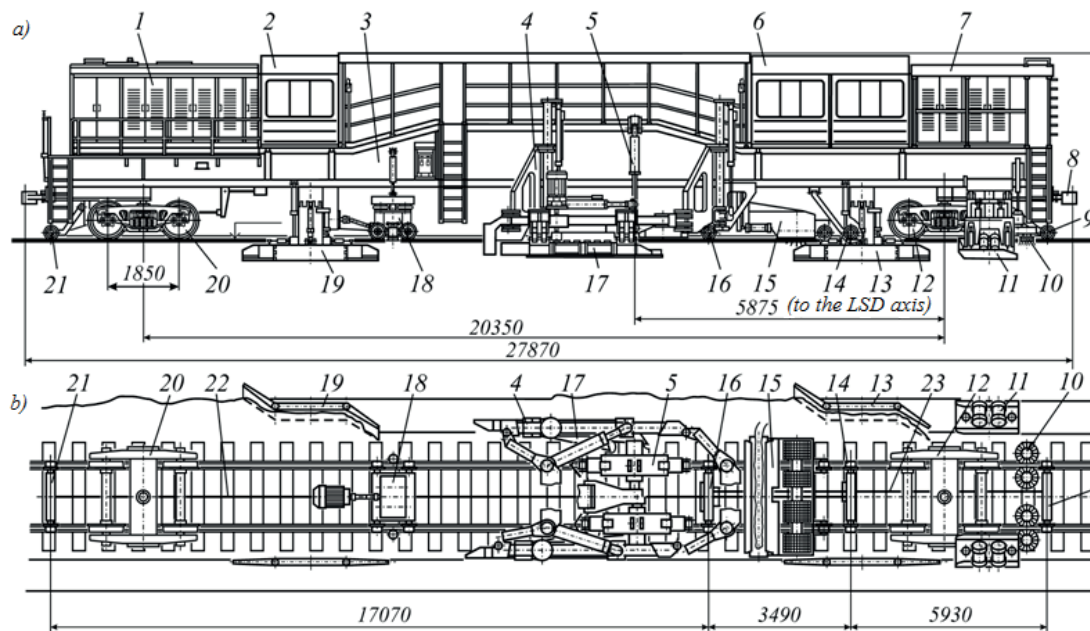


**Figure 1** The track renewal machine VPO-3-3000C: 1 - main and additional diesel-electric units of alternating current; 2 and 6 - front and rear control cabins, respectively; 3 - truss; 4 - mechanism for moving (suspension) of vibrating plates; 5 - LSD (lifting and straightening device); 7 - pumping station; 8 - automatic couplings; 9, 14, 16 and 21 - rear, intermediate and front carriages of the CTS, respectively; 10 - active rail brushes; 11 - seals of sloping shoulder and inter-track zones of the ballast; 14 and 20 - rear and front undercarriages (type 18-100), respectively; 13 - planners; 15 - ballast picker; 17 - main vibro-plates; 18 - working body of the track dynamic stabilization; 19 - dispenser; 22 and 23 - cable chords of the working and control CTS, respectively.

**Table 1** Availability of machines at the Akadyr mechanized distance

No.	Name	Amount, pcs.
1	Track renewal finishing machines VPO-3-3000	3
2	Ballasting machines ELB-4S	2
3	Track renewal trains VPR-1200	4
4	Straightening machines RB	2
5	Reclamation machines	3
6	Snow removal and snow cleaning machines	5
7	Motor platforms MPD	12
8	Track cranes UK	7
Total		38 machines

types of track repair including formation, compaction and stabilization of the ballast after deep cleaning of the crushed gravel. The machine is designed to perform a set of final works of technological processes of repair and construction of the track (Figure 1) [15].

At present, a fairly large number of track machines are operated at the Akadyr mechanized distance: availability of the machines is shown in Table 1.

The main economic effect from the operation of the VPO-3-3000 machine is increasing the operating time of sections of the railway track, because the more time it takes to repair the track, the less time it is operated.

The operating time of the VPO-3-3000, as statistics have shown, is reduced due to the unplanned repairs, as well as to scheduled maintenance of machines. This indicates

a significant loss of time for repairs within the “window”, disruption of the transportation process and economic losses in all the services (Figure 2).

Electromagnetic grippers used in the VPO-3-3000 machines are unreliable and lead to frequent failures (Figure 3). When the grate is discharged, additional time is required to recharge the working bodies and to eliminate distortions of the grate. As a result, the productivity and accuracy of the grating are reduced.

The discharge of the grating by electromagnetic grippers occurs for several reasons. On the way with the ballast metal inclusions adhere to the magnet. The electromagnetic field is dissipated; the lifting force of the gripper is reduced. It is necessary to clean the space from the ballast in the rail zone.

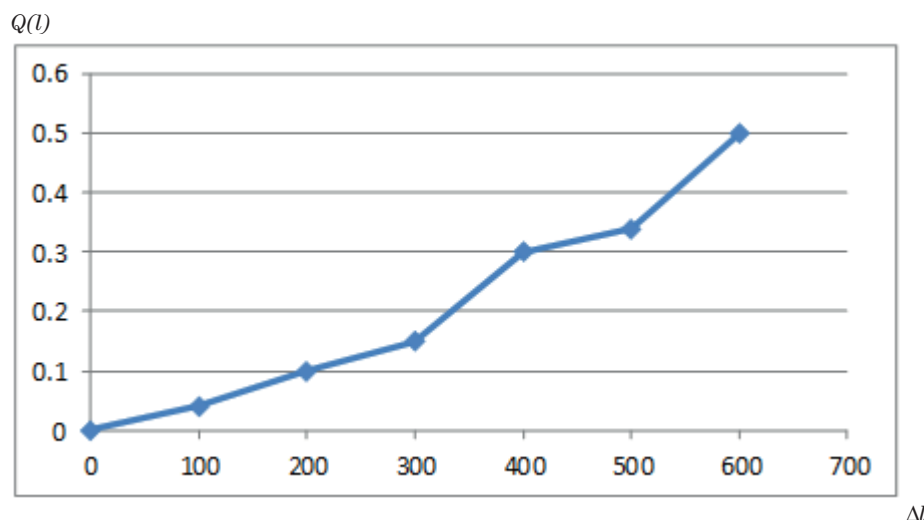


**Figure 2** Probability of the electromagnetic grippers failure  $Q(l)$  in terms of the operating time  $\Delta l$ , km



**Figure 3** Electromagnetic grippers of the VPO-3-3000 machine

Analysis of defects in work and technical failures due to track machines VPO-3-3000 shows that it is necessary to upgrade the weak components of the machine.

At the moment, the VPO-3-3000 machines with electromagnetic grippers are operating at the Akadyr machine-station.

To reduce unplanned failures and to increase reliability, in the VPO-3-3000 machines it is proposed to use the roller grippers instead of electromagnetic ones, which simplifies the operation of the machine (Figure 4).

### 3 Calculation and design of rail grips

The gripper design should permit the machine to pass the curved sections of the track and sections with changing gauge without jamming the rollers.

Important criteria for assessing design of the lifting machines are stock ratios for various parameters that determine their tension, deformability, bearing capacity and durability. Increasing the work resources leads to a sharp increase in both duration of the load and number of repetitions (cycles) of loading for some machines.

Accumulation of the long-term static and low-cycle damage in the material can lead to premature destruction of mechanisms and machines in general. Strength calculation should be based on the accurate assessment of stresses and strains, taking into account stress concentration, knowledge of material properties under similar loading conditions and use of the modern concepts of damage accumulation.

Studying the spatial stress state became possible in connection with development of the finite element method (FEM) that allows implementing well-developed procedures for solving the elastoplastic problem and the introduction of the CAE systems of sufficiently high efficiency. For this purpose, refined methods of calculation on a computer have been developed.

When designing a lifting machine, the designer relies on his experience, developing a new or modifying the known structure and then carries out a verification calculation for strength. This leads to multiple repetitions of calculations and requires significant costs when selecting the best option. The development of a method for calculating the lifting-straightening device (hereinafter referred to as the LSD), taking into account the working conditions

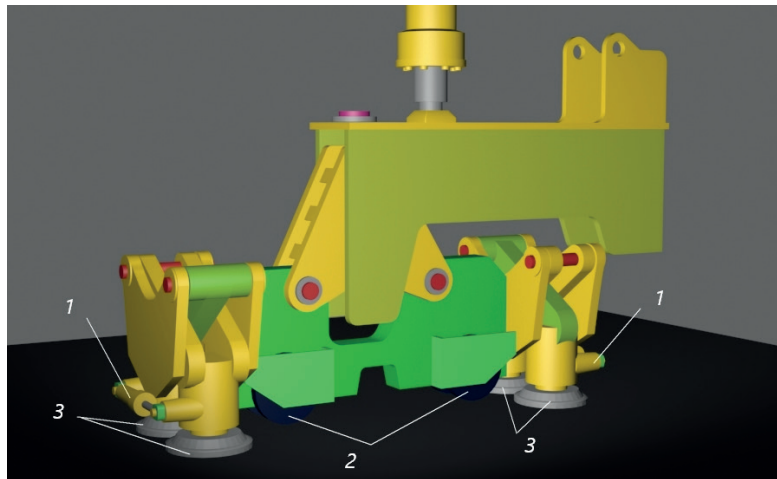


**Figure 4** Roller rail gripper: 1 - gripper drive hydraulic cylinder; 2 - straightening roller; 3 - pickup roller

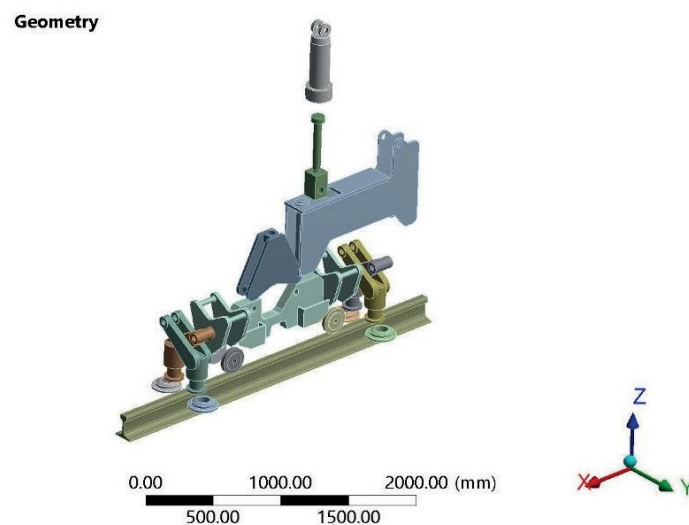


**Figure 5** Three-dimensional assembly model of the LLD (lifting-leveling device) design

and strength requirements, implemented in the form of a computer-aided design system, is an urgent task. Solving this problem allows identifying the relationship of various requirements for strength, stiffness, working parameters of the structure and characteristics of the material with the optimal design. The design is to take into account not only static but also dynamic characteristics of machines, with detuning from critical loads in the operating range. In this regard, it is necessary to calculate initially the structure strength and rigidity.

In assessing strength of the structural elements of the lifting machines' experimental research methods are important. The main ones are testing structural elements at experimental stands. Systems for automatic control of stands allow developing cyclic loads, which makes it possible to study durability of structures. Such tests require additional calculations related to determining the type of loading cycle, the number of cycles, safety factors, etc.

The strength assessment methods, used in scientific and industrial practice, developed based on the numerical and analytical studies, cannot be reliable without any additional experimental studies.

Below there is a calculation of the structural elements strength of the LSD during its operation, in the AnsysWB software package

The AnsysWB analysis system consists of a lot of modules. The StaticStructural module was selected for implementation of this calculation. First, a three-dimensional assembly model of the switchgear design was built in the Component Systems Geometry (DesignModeler) (Figure 5).

The Static Structural project consists of six sections: geometry, materials, coordinate systems, connections, mesh, static structural.

In the geometry section, a three-dimensional (one-dimensional, two-dimensional) model is loaded, in which materials are assigned to each assembly node. In addition, where one can change the type of material, that is, to take a deformable or an absolutely rigid one.

In the materials section one can directly view and change the parameters of the materials.

The coordinate systems item allows setting and adjusting (moving, rotating) the coordinate system by switching the Cartesian and cylindrical coordinate systems.



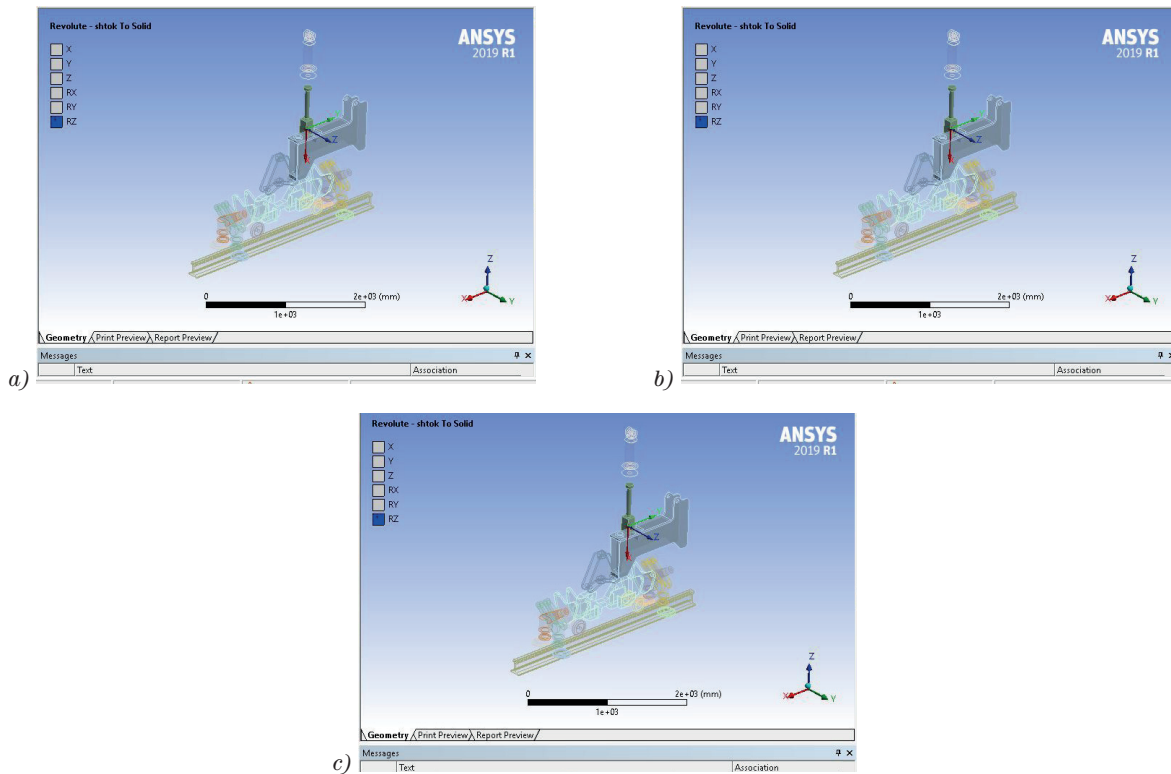


Figure 6 Connections configuration

The model has contact connections, which lead to solution of a nonlinear problem. All the nonlinear problems have no convergence of the solution. To improve the convergence of calculation, it is necessary to eliminate the motion of loose bodies, that is, before the calculation, it is necessary to ensure that there is a contact between all the parts that must be in contact. This is achieved by moving the bodies, adding a shift on the contact surfaces (contact offset) or using the damping mechanism (stabilization damping), as well as by setting friction on the contacting surfaces.

If there is also no convergence of calculation, then you should reduce the stiffness of the contact elements (smooth application of the load and decrease of the contact pairs stiffness provide solving to 90% of problems with the convergence of the calculation); seal the grid in the contact zone to reduce the proportion of elements in which the contact status changes during the calculation.

Building a three-dimensional model was carried out in the geometry section of this module. Methods of changing coordinates and Boolean operations were used.

In the connections environment, joint (Figure 6) and contact pairs (contacts) are configured (Figure 7).

The vertical track displacement is a function of foundation system stiffness; therefore, if the displacement is known, then the system parameters (e.g., smeared values representing the entire system) can be back-calculated by using an appropriate foundation model [16].

The connections configuration is performed according to the degrees of freedom nature. Figure 8 w shows the graph of the nonlinear problem convergence.

A simple and widely accepted model for displacement of a railway track at low frequency is a beam on an elastic foundation [17].

The fourth theory of strength is the most often called the Mises criterion. It is based on the following hypothesis: strength of an element in the combination stress state is considered exhausted (i.e., the ultimate stress state occurs) if the specific potential energy of its shape change reaches the limit determined from simple tensile experiments [18]. Results of the strength calculation are given in Table 2.

According to Mises, stress is expressed as:

$$\sigma_{vonMises} = \sqrt{\frac{1}{2}[(\sigma_1 - \sigma_2)^2 + (\sigma_2 - \sigma_3)^2 + (\sigma_3 - \sigma_1)^2]}, \quad (1)$$

where  $\sigma_1, \sigma_2, \sigma_3$  are the principal stresses.

Strength with the  $n$  margin is provided under the condition:

$$\begin{aligned} & \frac{1}{\sqrt{2}} \sqrt{(\sigma_1 - \sigma_2)^2 + (\sigma_2 - \sigma_3)^2 + (\sigma_3 - \sigma_1)^2} = \\ & = \frac{\sigma_{lim}}{n} = [\sigma]. \end{aligned} \quad (2)$$

The condition of strength takes the final form:

$$\begin{aligned} \sigma_{vonMises} &= \frac{1}{\sqrt{2}} \sqrt{(\sigma_1 - \sigma_2)^2 + (\sigma_2 - \sigma_3)^2 + (\sigma_3 - \sigma_1)^2} \\ &\leq [\sigma], \end{aligned} \quad (3)$$

where  $[\sigma] = \frac{\sigma_{lim}}{n}$  is admissible stress.

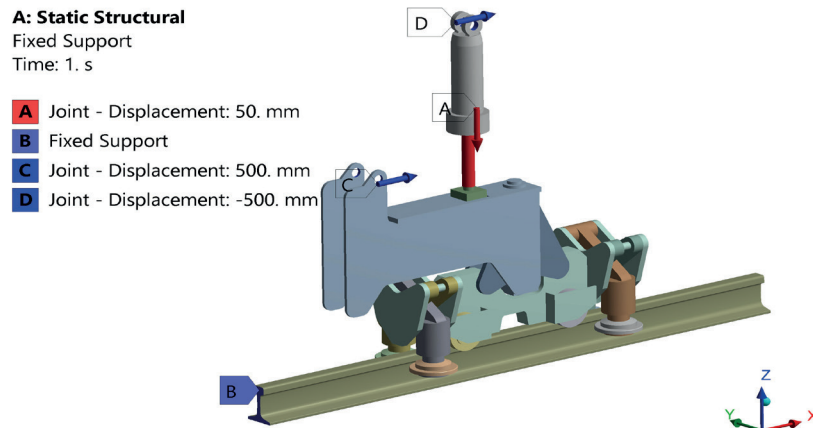


Figure 7 Boundary conditions of the design

Table 2 Results of the strength calculation

Parts	Material	Mises stress $\sigma_{\text{vonMises}}$ , MPa	Admissible stress $\sigma_{\text{adm}}$ , MPa
R75 rail	M76	124	900/1.5=600
Bracket arm	30HGSA	378	400
Right gripper	Steel 45	80	240
Left gripper	Steel 45	117	240
Stock	30HGSA	252	400
Cylinder	30HGSA	162	400
Support rollers	Steel 45	210	240



Figure 8 Graph of the nonlinear problem convergence

The fourth theory of strength, as well as the third one, is well confirmed experimentally, as the theory of the material transition to the plastic state and alongside with the third theory of strength, it is widely used to calculate strength of parts made of plastic materials.

The following boundary conditions were adopted (Figure 7): A is the connection of the rod to the cylinder, in which all the degrees of freedom are limited except for the translational movement along the X axis (red down arrow); B is one end of the rail that is pinched (limited movement in all directions); C and D is a movable cylindrical hinge (there is a single movement and rotation).

Equivalent stresses, arising from operational loads, do not exceed the admissible stress.

Neglecting inertial effects and track roughness, this can be used to model the deflection due to a single static

load (Figure 9(a)), a moving load or a train of moving loads (Figure 9(b)) [19].

The static displacement  $w$ , at a distance  $x$  along a beam, with bending stiffness  $EI$  on an elastic foundation with a system support modulus (stiffness per unit length)  $k$ , has the governing equation:

$$EI \frac{d^4 w(x)}{dx^4} + kw(x) = 0. \quad (4)$$

The deflection due to a single load  $F$  acting at  $x = 0$  (Figure 9(a)) has the solution:

$$w(x) = \frac{F}{2kL} e^{-\frac{|x|}{L}} \cdot \left( \cos\left(-\frac{|x|}{L}\right) + \sin\left(-\frac{|x|}{L}\right) \right), \quad (5)$$

where  $L$  is a characteristic length:

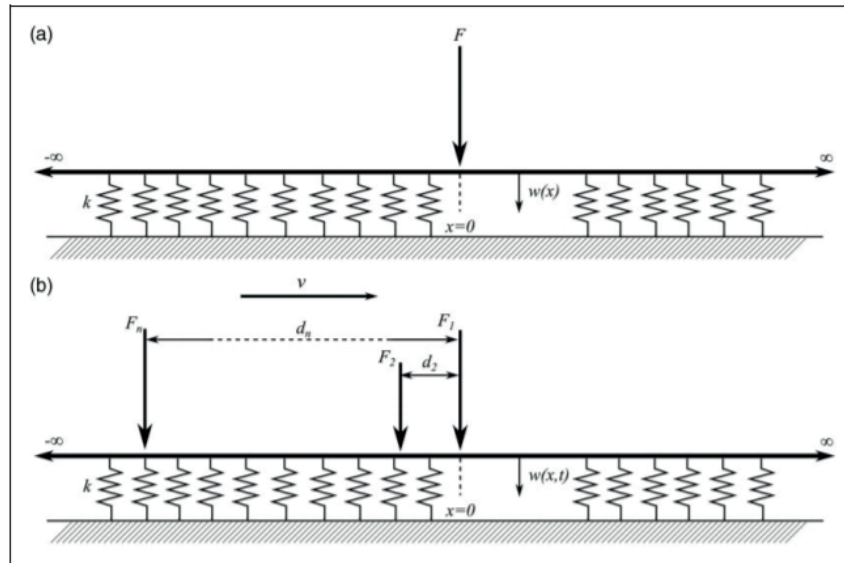


Figure 9 Beam on an elastic foundation subjected to (a) a static point load and (b) a train of moving loads

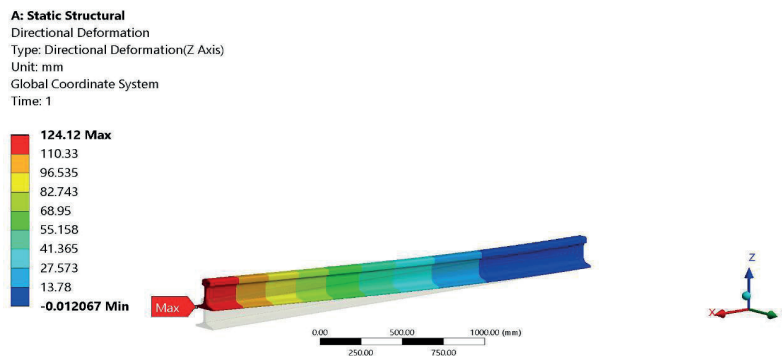


Figure 10 Vertical strain of the R75 rail

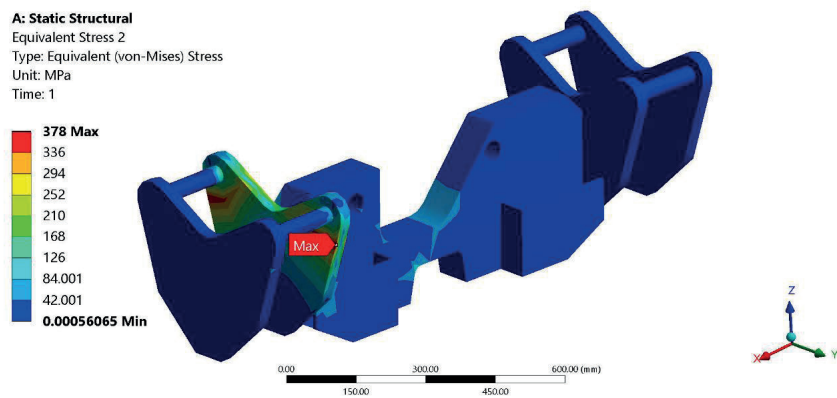


Figure 11 Stress distribution according to Mises

$$L = \sqrt[4]{\frac{4EI}{k}}.$$

A point on the track, subjected to a load moving at a constant speed  $v$ , experiences this deflection as a function of time  $t = x/v$ . The solution for the time-varying displacement of the track at a point, due to a train of moving loads (Figure 9 (b)), each separated from the first

load by a distance  $x_n$ , can be found by summing the effect of each wheel load:

$$w(t) = \sum_n \frac{F}{2kL} e^{-\frac{|t - \frac{x_n}{v}|}{L}} \cdot \left( \cos\left(-\frac{|t - \frac{x_n}{v}|}{L}\right) + \sin\left(-\frac{|t - \frac{x_n}{v}|}{L}\right) \right). \quad (7)$$

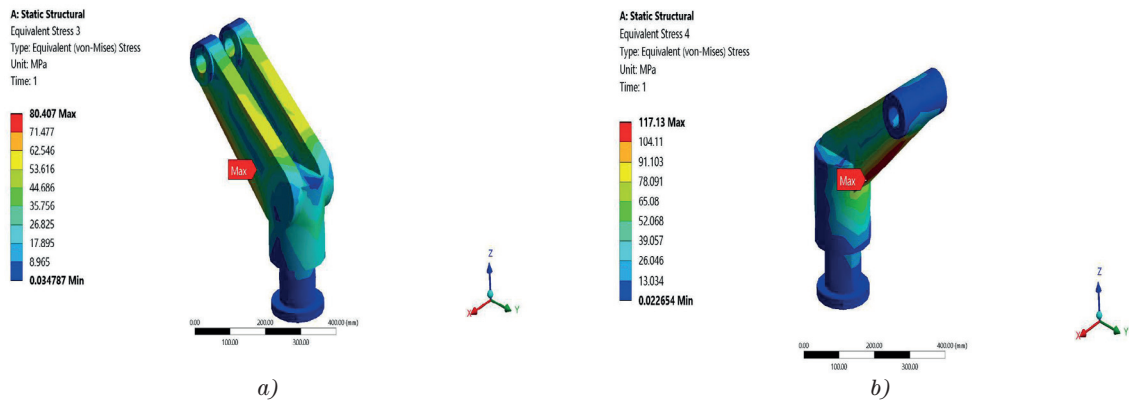


**Figure 12** Stress distribution on grippers according to Mises: a) front right gripper; b) front left gripper

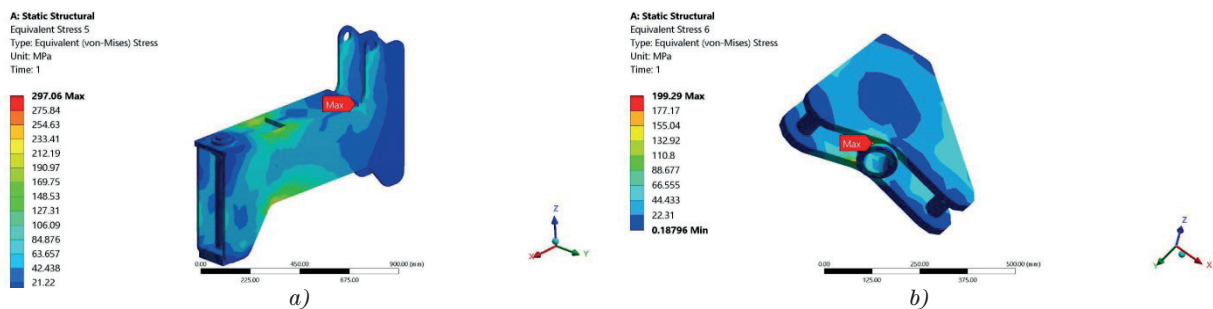


**Figure 13** Stresses according to Mises: a) front right gripper; b) front left gripper

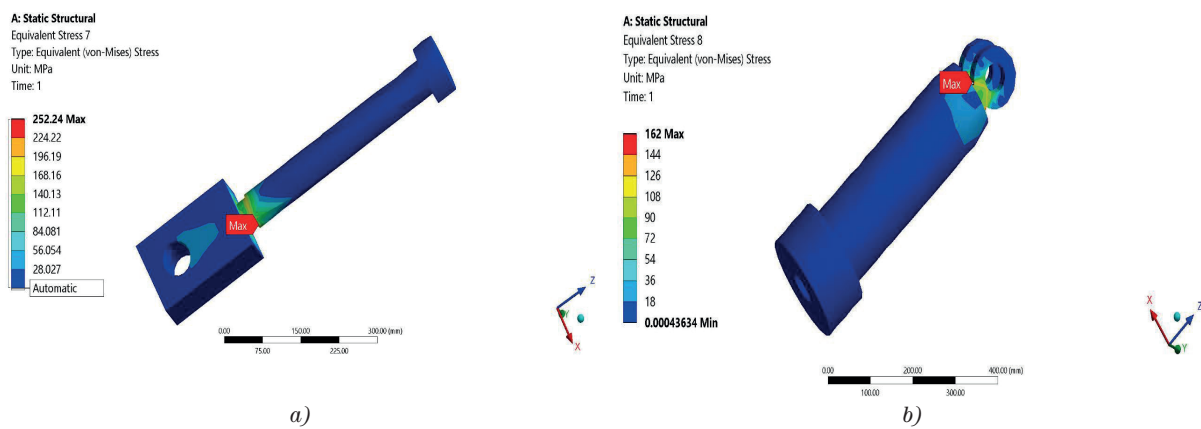


**Figure 14** Stress distribution of hydraulic cylinder according to Mises: a) rod; b) cylinder

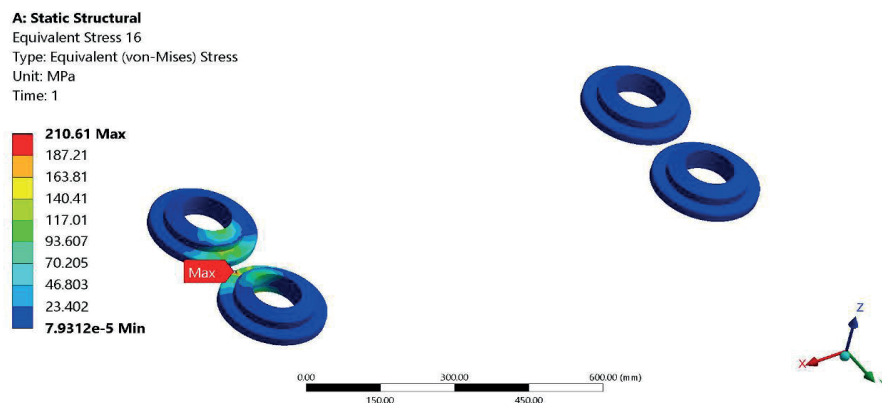


**Figure 15** Stress distribution of the support roller according to Mises



If measurements are made on the sleeper instead of on the rail, the sleeper deflection  $w_s$  has the same pattern but with a reduced amplitude that depends on ratio of the rail pad modulus  $k_p$  to the total system support modulus  $k$

$$w_x = w \left( 1 - \frac{k}{k_p} \right). \quad (8)$$

As a result of calculation, the nature of the Mises stress change and strain in elements during the operation of the LSD were obtained.

Figure 10 shows changing the vertical strain of the R75 rail.

From the strain pattern and the strain value indicator, one notes that the vertical strain at the end of the rail was 124mm, which does not exceed the maximum permissible value.

Then, in Figure 11, one can observe symmetrical stress concentrations of 378 MPa on the grippers enclosing structure, which requires use of a material that provides strength for this design.

Figures 12 a, b show stress distribution according Mises of the most loaded front grippers. In these elements, strength is provided with a margin. On the left gripper, the stress is higher than on the right one.

The largest stress concentrations, according to Mises in Figures 13 a, b, arise due to abrupt transitions in the geometry of elements. This problem is fixed by the geometry adjustment.

Figures 14 a, b show the stress state of the hydraulic cylinder.

The maximum stress concentration in Figure 13 a is explained by a sharp transition.

Figure 15 shows the contact stresses of the support roller.

This stress can be varied by changing the gripping power of the R75 rail. Strength and rigidity of the LSD design are provided.

#### 4 Conclusions

1. For the first time, the spatial stress-strain state of a lifting-straightening device has been studied.
2. The numerical and analytical strength assessment, used in scientific and industrial practice, cannot be reliable without any additional experimental studies.
3. Accumulation of the long-term static and low-cycle damage in the material can lead to premature destruction of the machines.
4. Strength and rigidity of the lifting-straightening device is provided overall.
5. The convergence of the nonlinear (contact) problem is achieved by eliminating the motion of loose bodies, reducing the stiffness of the contact elements and by sealing the CEs in the contact zone.

#### References

- [1] CECILIA, V., ISABEL, M. R., RUI, C. Integer programming to optimize tamping in railway tracks as preventive maintenance. *Journal of Transportation Engineering* [online]. 2011, **138**(1), p. 123-131. ISSN 2473-2907, eISSN 2473-2893. Available from: [https://doi.org/10.1061/\(ASCE\)TE.1943-5436.0000296](https://doi.org/10.1061/(ASCE)TE.1943-5436.0000296)
- [2] INDRARATNA, B., THAKUR, P. K., VINOD, J. S. Experimental and numerical study of railway ballast behavior under cyclic loading. *International Journal of Geomechanics* [online]. 2010, **10**(4), p. 136-144. ISSN 1532-3641, eISSN 1943-5622. Available from: [https://doi.org/10.1061/\(ASCE\)GM.1943-5622.0000055](https://doi.org/10.1061/(ASCE)GM.1943-5622.0000055)
- [3] ZHAI, W. M., WANG, K.Y., LIN, J. H. Modelling and experiment of railway ballast vibrations. *Journal of Sound and Vibration* [online]. 2004, **270**(4), p. 673-683. ISSN 0022-460X. Available from: [https://doi.org/10.1016/S0022-460X\(03\)00186-X](https://doi.org/10.1016/S0022-460X(03)00186-X)
- [4] NISSEN, A. *Development of life cycle cost model and analyses for railway switches and crossings*. Doctoral thesis. Lulea: Lulea University of Technology, 2009. ISSN 1402-1544, ISBN 978-91-7439-026-1.
- [5] Rules of technical operation, maintenance and repair of railway tracks / *Pravila tekhnicheskoy ekspluatatsii, tekhnicheskogo obsluzhivaniya i remonta zheleznodorozhnykh putey* (in Russian). Astana, 2011.
- [6] LU, M., MCDOWELL, G. R. Discrete element modelling of railway ballast under monotonic and cyclic triaxial loading. *Geotechnique* [online]. 2010, **60**(6), p. 459-467. ISSN 0016-8505, eISSN 1751-7656. Available from: <https://doi.org/10.1680/geot.2010.60.6.459>
- [7] AUGUSTIN, G., GUDEHUS, G., HUBER, G., SCHUNEMANN, A. Numerical model and laboratory tests on settlement of ballast track. In: *System dynamic and long-term behaviour of railway vehicles, track and subgrade* [online]. POPP, K., SCHIEHLEN, W. (Eds.). Berlin Heidelberg: Springer-Verlag, 2003. eISBN 978-3-540-45476-2, p. 317-366. Available from: <https://doi.org/10.1007/978-3-540-45476-2>
- [8] KIM, Y.-M. A Granular motion simulation by discrete element method. *Journal of Mechanical Science and Technology* [online]. 2008, **22**, p. 812-818. ISSN 1738-494X, eISSN 1976-3824. Available from: <https://doi.org/10.1007/s12206-008-0112-7>
- [9] HUANG, H., TUTUMLUER, E. Discrete Element Modeling for fouled railroad ballast. *Construction and Building Materials* [online]. 2011, **25**(8), p. 3306-3312. ISSN 0950-0618. Available from: <https://doi.org/10.1016/j.conbuildmat.2011.03.019>

- [10] YAN, Y., JI, S. Discrete element modeling of direct shear tests for a granular material. *International Journal for Numerical and Analytical Methods in Geomechanics* [online]. 2010, **34**(9), p. 978-990. eISSN 1096-9853. Available from: <https://doi.org/10.1002/nag.848>
- [11] FISCHER, S., JUHASZ, E. Railroad ballast particle breakage with unique laboratory test method. *Acta Technica Jaurinensis* [online]. 2019, **12**(1), p. 26-54. eISSN 2064-5228. Available from: <https://doi.org/10.14513/actatechjaur.v12.n1.489>
- [12] IZVOLT, L., SESTAKOVA, J., SMALO, M. Analysis of results of monitoring and prediction of quality development of ballasted and ballastless track superstructure and its transition areas. *Communications - Scientific Letters of the University of Zilina* [online]. 2016, **18**(4), p. 19-29. Available from: <http://komunikacie.uniza.sk/index.php/communications/article/view/284>
- [13] KOVALCHUK, V., KOVALCHUK, Y., SYSYN, M., STANKEVYCH, V., PETRENKO, O. Estimation of carrying capacity of metallic corrugated structures of the type multiplate mp 150 during interaction with backfill soil. *Eastern European Journal of Enterprise Technologies* [online]. 2018, **1**(91), p. 18-26. ISSN 1729-3774, eISSN 1729-4061. Available from: <https://doi.org/10.15587/1729-4061.2018.123002>
- [14] NABOCHENKO, O., SYSYN, M., KOVALCHUK, V., KOVALCHUK, Y., PENTSACK, A., BRAICHENKO, S. Studying the railroad track geometry deterioration as a result of an uneven subsidence of the ballast layer. *Eastern-European Journal of Enterprise Technologies* [online]. 2019, **97**(1), p. 50-59. ISSN 1729-3774, eISSN 1729-4061. Available from: <https://doi.org/10.15587/1729-4061.2019.154864>
- [15] POPOVICH, M. V., BUGAYENKO, V. M. *Track machines. Complete course / Putevyye mashiny. Polnyy kurs* (in Russian). Moscow: Transport, 2009. ISBN 978-5-9994-0003-1
- [16] MURRAY, C. A., TAKE, W. A., HOULT, N. A. Measurement of vertical and longitudinal rail displacements using digital image correlation. *Canadian Geotechnical Journal*. 2014, **52**, p. 141-55. ISSN 1208-6010.
- [17] TIMOSHENKO, S., LANGER, B. F. Stresses in railroad track. *Transactions of the American Society of Mechanical Engineers*. 1932, **54**, p. 277-293. ISSN 0021-8936, eISSN 0097-6822.
- [18] GREBENNIKOV, M. N. *Theory of strength. Combination resistance*. Tutorial. National Aerospace University H.E. Zhukovsky "Kharkiv Aviation Institute", 2016. ISBN 978-966-662-503-1.
- [19] MILNE, D., PEN, L. L., THOMPSON, D., POWRIE, W. Automated processing of railway track deflection signals obtained from velocity and acceleration measurements. *Proceedings of the Institution of Mechanical Engineers, Part F: Journal of Rail and Rapid Transit* [online]. 2018, **232**(8), p. 2097-2110. ISSN 0954-4097, eISSN 2041-3017. Available from: <https://doi.org/10.1177/0954409718762172>